

Full Bayesian Analysis of the MEG Inverse Problem with ℓ^p -norm Priors

Toni Auranen*, Apoo Nummenmaa*, Matti S. Hämäläinen†, Iiro P. Jääskeläinen*†, Jouko Lampinen*, Aki Vehtari*, and Mikko Sams*

* Laboratory of Computational Engineering, Helsinki University of Technology, Finland (correspondence: Toni.Auranen@hut.fi)

† Massachusetts General Hospital, Harvard Medical School, Athinoula A. Martinos Center for Biomedical Imaging, Charlestown, MA, USA

Introduction

We performed a full Bayesian analysis of the ℓ^p -norm prior model in MEG source localization. Using Markov chain Monte Carlo (MCMC) methods, numerical samples were obtained from the joint posterior distribution of the parameters (simulated neural currents) and hyperparameters (ℓ^p -norm order, p , and prior width, ν) after which inverse estimates for the sources were computed.

- Minimum-norm [1] and minimum-current [2] estimates (MNE and MCE) are widely used distributed source estimating methods in MEG/EEG research
- With Bayesian interpretation these models have a Gaussian likelihood for measurements and an ℓ^p -norm (Eq. 1) prior for the sources

$$\|s\|_p = \left(\sum_i |s_i|^p \right)^{1/p} \quad (1)$$

- MCE (ℓ^1 -norm prior for the neural currents) produces focal estimates whereas MNE (ℓ^2 -norm) produces more diffuse estimates
- In Bayesian sense [3], the choice of the norm order, p , is subject to uncertainty and it can be treated as an unknown variable; the value of p is also more or less arbitrary as any value between 1 and 2 could be used

Methods

Gaussian noise was added to the measurements that were simulated using a discretized forward model. The model was embedded in a realistic framework of a real MEG device. The method of slice sampling was used to obtain numerical samples from the posterior distribution.

- A single-compartment MRI-based boundary-element model was utilized and possible source locations were restricted to the gray-white matter boundary while source orientations were constrained to be normal to the cortex [4]
- Three differently sized source spaces were used, containing roughly 1600, 3200 and 6400 discretization points
- Measurements (Fig. 1) were created with a source space of about 32000 points so that the effect of inverse crime was reduced by not using the same grid size for solutions

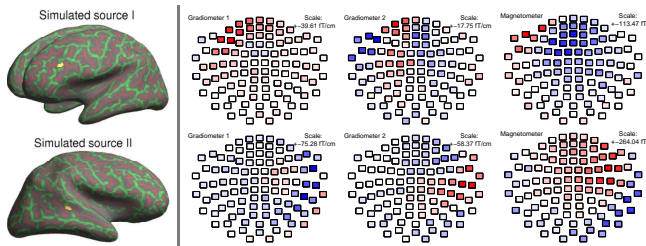


Figure 1: Two simulated sources (I & II on the left prefrontal and right auditory cortex, correspondingly) are plotted with yellow on an inflated gray-white matter boundary. The green color depicts gyri and red color sulci, respectively. The measurements calculated with the forward model for source I are on the upper row and for source II on the lower row. The measurements comprise of 306 sensors (two orthogonal gradiometers and one magnetometer) in 102 different locations. The sensor grid is viewed from the top, nose pointing up.

- Quasistatic approximation of the Maxwell's equations and discretization leads to a discrete linear forward model, where \mathbf{b} stands for measurements, \mathbf{A} for gain matrix, \mathbf{s} for source current vector, and \mathbf{n} for Gaussian noise:

$$\mathbf{b} = \mathbf{A}\mathbf{s} + \mathbf{n} \quad (2)$$

- For the currents, the posterior distribution probability is, according to Bayes' rule [3], defined by the likelihood and prior terms and a normalization constant $p(\mathbf{b})$:

$$p(\mathbf{s}|\mathbf{b}) = \frac{p(\mathbf{b}|\mathbf{s}) \cdot p(\mathbf{s})}{p(\mathbf{b})} \quad (3)$$

- In statistical terms Eq. 2 can be written as a linear regression model and when combined with the prior in Eq. 1, Eq. 3 is proportional to the following, where ν and p are parametrized according to [5, Ch. 3.2.1] and $\{C_1, C_2\}$ are normalizing factors:

$$\exp(-(\mathbf{b} - \mathbf{A}\mathbf{s})^T \mathbf{C}_1^{-1} (\mathbf{b} - \mathbf{A}\mathbf{s})) \cdot C_1(\beta(p), \nu) \cdot \exp(-C_2(\beta(p)) \cdot (\|s/\nu\|)^{\beta(p)}) \quad (4)$$

- MCMC method of slice sampling [6] was chosen in order to reduce correlations between the source current parameters, \mathbf{s} , and prior width, ν

Results

At least 5000 samples were drawn from the posterior. The inverse estimates (Fig. 2) were computed as the posterior expectation values of the currents integrated over the hyperparameters p and ν for different grid sizes. The posterior distributions of p and ν are shown in Fig. 3.

- Convergence diagnostics and time series analysis were used to verify that the convergence of the sampler was plausible

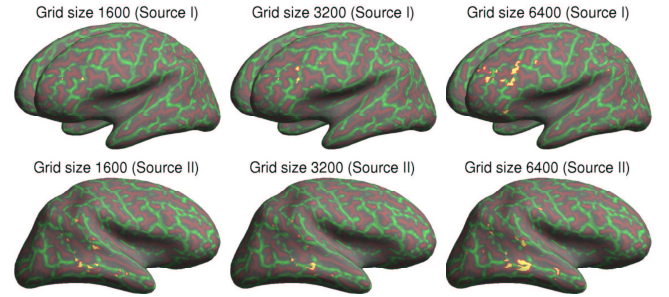


Figure 2: The inverse estimates were interpolated on the original (~32000 source points) inflated cortical mantle. The yellow color reflects all those source points whose estimated amplitude exceeds 25% of the maximum value. The estimates were calculated for 3 different grid sizes for both sources (I & II).

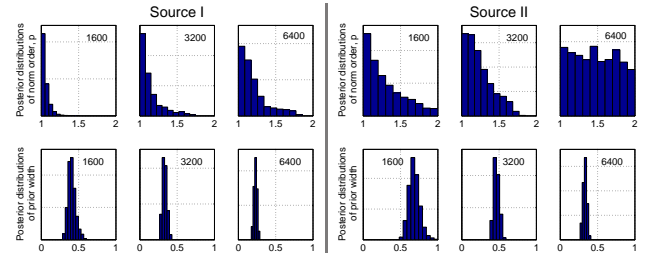


Figure 3: The histograms of posterior samples of the hyperparameters p and ν for different grid sizes are on the top and bottom row, correspondingly. The six leftmost subfigures are for source I and those on the right for source II. The distribution of p is somewhat diffuse and depends both on the source and grid size used. This suggests that fixing it to some predefined value (e.g., 1 or 2) easily leads to overfitted estimates.

Conclusions

The method is computationally very heavy but fairly automatic as it requires only little or no tuning as all parameters and hyperparameters are estimated from the data without manual interaction. It also seems clear that the norm order of the ℓ^p -norm prior should not be chosen *ad hoc*, but should be inferred from the data. To improve localization, we are currently studying the use of spatial priors.

- With cortical orientation constraint the small grid discretization sizes may be too limited for empirical investigations; with the cost of computationally unconstrained grids might increase localization accuracy
- For larger discretization sizes the assumption of independent currents begins to break and the model requires some spatial priors

References

- [1] Matti S. Hämäläinen and Risto J. Ilmoniemi. Interpreting measured magnetic fields of the brain: Estimates of current distributions. Technical Report TKK-F-A559, Helsinki University of Technology, Department of Technical Physics, 1984.
- [2] K. Uutela, M. Hämäläinen, and E. Somersalo. Visualization of magnetoencephalographic data using minimum current estimates. *NeuroImage*, 10:173–180, 1999.
- [3] Andrew Gelman, John B. Carlin, Hal S. Stern, and Donald B. Rubin. *Bayesian Data Analysis*. Chapman & Hall/CRC, second edition, 2003.
- [4] Anders M. Dale and Martin I. Sereno. Improved localization of cortical activity by combining EEG and MEG with MRI cortical surface reconstruction: A linear approach. *Journal of Cognitive Neuroscience*, 5(2):162–176, 1993.
- [5] George E. P. Box and George C. Tiao. *Bayesian Inference in Statistical Analysis*. John Wiley and Sons, Inc., 1973.
- [6] Radford M. Neal. Slice sampling. *The Annals of Statistics*, 31(3):705–767, 2003.